Insect Biochemistry and Molecular Biology 43 (2013) 1161–1171

Contents lists available at ScienceDirect

Insect Biochemistry and Molecular Biology

journal homepage: www.elsevier.com/locate/ibmb

Gustatory receptor expression in the labella and tarsi of *Aedes aegypti*

Jackson T. Sparks [a], Bryan T. Vinyard [b], Joseph C. Dickens [a,*]

[a] United States Department of Agriculture, Agricultural Research Service, Henry A. Wallace Beltsville Agricultural Research Center, Plant Sciences Institute, Invasive Insect Biocontrol and Behavior Laboratory, Beltsville, MD 20705, USA
[b] United States Department of Agriculture, Agricultural Research Service, Henry A. Wallace Beltsville Agricultural Research Center, Biometrical Consulting Service, Beltsville, MD, USA

ARTICLE INFO

Article history:
Received 26 July 2013
Received in revised form
25 September 2013
Accepted 10 October 2013

Keywords:
Gustatory receptor
Taste
Aedes aegypti
Labella
Tarsi

ABSTRACT

The yellow-fever mosquito, *Aedes aegypti*, infects a growing number of people every year with dengue, yellow fever and chikungunya viruses. Contact chemoreception in mosquitoes influences a number of behaviors including host-selection, oviposition and feeding. While these behaviors are in many instances well documented, the molecular mechanisms mediating them are not well understood. Here we report the results of sequencing total messenger RNA in the labella and tarsi of both male and female *Ae. aegypti* to reveal Gustatory Receptor (GR) gene expression profiles in these major gustatory appendages. Gene expression levels in each tissue were verified by RT-qPCR. We discuss potential functions for the GRs revealed here by considering homologous GRs in other insects. Specific GRs provide molecular targets for modification of gustatory-mediated behaviors in this important disease vector.

Published by Elsevier Ltd.

1. Introduction

Aedes aegypti (L.) (Diptera: Culicidae) is an important disease vector, contributing to the spread of dengue, yellow fever, chikungunya and West Nile viruses. Perhaps most alarming is the deadly dengue virus, as female *Ae. aegypti* infect between 50 and 390 million people yearly through blood-meal mediated viral transmission (Guzman et al., 2010; Beatty et al., 2011; Bhatt et al., 2013). The production of a dengue vaccine is challenging, and unpredictable viral mutation threatens long-term efficacy (Barban et al., 2012; Sabchareon et al., 2012; Wallace et al., 2013). Thus, prevention of mosquito bites remains one of the chief strategies to break this viral transmission cycle. Deterrents such as DEET can reduce the chances of mosquito bites and prevent disease transmission (Debboun and Strickman, 2013). Central to the discovery of other useful deterrents is the identification of the receptor molecules mediating responses to such compounds. While *Ae. aegypti* olfactory receptors have recently been implicated in the detection of volatile DEET (DeGennaro et al., 2013), receptors involved in gustatory responses to DEET and other deterrent compounds (Sanford et al., 2013) have not been determined for mosquitoes.

The repertoire of genes involved in insect gustatory reception is diverse (Liu et al., 2003; Lin et al., 2005; Al-Anzi et al., 2006; Fischler et al., 2007; Mitri et al., 2009; Cameron et al., 2010; Chen et al., 2010; Croset et al., 2010; Kim et al., 2010; Zhang et al., 2013) and includes the large, divergent gene family of Gustatory Receptors (GRs) (Clyne et al., 2000; Dunipace et al., 2001; Scott et al., 2001; Robertson et al., 2003; Isono and Morita, 2010). Membrane-bound insect GRs are generally expressed in gustatory receptor neurons (GRNs) whose dendritic processes innervate sensory hairs or sensilla distributed on the paired labella, labrum, inner mouthparts, wing margins, genitalia, and tarsal segments of the legs (Dunipace et al., 2001; Scott et al., 2001; Thorne et al., 2004; Wang et al., 2004; Dahanukar et al., 2007). The porous tip of these sensilla allows chemicals to come into contact with GRNs within the sensillar lumen (Stocker, 1994). At this interface, individual or complexes of GRs are selectively activated by chemicals, leading to neuronal responses resulting in action potentials that are carried by axonal processes to the primary gustatory centers of the brain or other central ganglia (Miyazaki and Ito, 2010). Here information from various sensory modalities is integrated, thus enabling insects, including mosquitoes, to assess and respond to their chemical environment.

Mosquitoes locate potential food sources and mates at a distance using olfactory, visual, and other cues like temperature and humidity (Peterson and Brown, 1952; Laarman, 1958; Bidlingmayer and Hem, 1980; Bowen, 1991; Clements, 1992; Klun et al., 2013). Upon landing, sensory hairs of the tarsal segments make the first

* Corresponding author. USDA, ARS, BARC, PSI, IIBBL, Bldg. 007, Rm. 030, 10300 Baltimore Avenue, Beltsville, MD 20705, USA. Tel.: +1 301 504 8957; fax: +1 301 504 6580.
E-mail addresses: joseph.dickens@ars.usda.gov, jdickdickens@comcast.net (Joseph C. Dickens).

0965-1748/$ – see front matter Published by Elsevier Ltd.
http://dx.doi.org/10.1016/j.ibmb.2013.10.005

Report Documentation Page

Form Approved
OMB No. 0704-0188

1. REPORT DATE	2. REPORT TYPE	3. DATES COVERED
OCT 2013		**00-00-2013 to 00-00-2013**

4. TITLE AND SUBTITLE	5a. CONTRACT NUMBER
Gustatory receptor expression in the labella and tarsi of Aedes aegypti	5b. GRANT NUMBER
	5c. PROGRAM ELEMENT NUMBER
6. AUTHOR(S)	5d. PROJECT NUMBER
	5e. TASK NUMBER
	5f. WORK UNIT NUMBER

7. PERFORMING ORGANIZATION NAME(S) AND ADDRESS(ES)	8. PERFORMING ORGANIZATION REPORT NUMBER
U.S. Department of Agriculture, Agricultural Research Service,Henry A. Wallace Beltsville Agricultural Research Center, Plant Sciences Inst,Invasive Insect Biocontrol and Behavior Laboratory,Beltsville,MD,20705	
9. SPONSORING/MONITORING AGENCY NAME(S) AND ADDRESS(ES)	10. SPONSOR/MONITOR'S ACRONYM(S)
	11. SPONSOR/MONITOR'S REPORT NUMBER(S)

12. DISTRIBUTION/AVAILABILITY STATEMENT

Approved for public release; distribution unlimited

13. SUPPLEMENTARY NOTES

14. ABSTRACT

The yellow-fever mosquito, Aedes aegypti, infects a growing number of people every year with dengue yellow fever and chikungunya viruses. Contact chemoreception in mosquitoes influences a number of behaviors including host-selection, oviposition and feeding. While these behaviors are in many instances well documented, the molecular mechanisms mediating them are not well understood. Here we report the results of sequencing total messenger RNA in the labella and tarsi of both male and female Ae. aegypti to reveal Gustatory Receptor (GR) gene expression profiles in these major gustatory appendages. Gene expression levels in each tissue were verified by RT-qPCR. We discuss potential functions for the GRs revealed here by considering homologous GRs in other insects. Specific GRs provide molecular targets for modification of gustatory-mediated behaviors in this important disease vector.

15. SUBJECT TERMS

16. SECURITY CLASSIFICATION OF:			17. LIMITATION OF ABSTRACT	18. NUMBER OF PAGES	19a. NAME OF RESPONSIBLE PERSON
a. REPORT	b. ABSTRACT	c. THIS PAGE			
unclassified	**unclassified**	**unclassified**	**Same as Report (SAR)**	**11**	

contact assessment of the sugar source or blood-host. This initial gustatory assessment is followed by a brief exploratory phase wherein the labellum repeatedly contacts the surface of the plant or animal host to further evaluate nutritive resources (Clements, 1992). Contact gustatory reception may also be used by mosquitoes to assess the social status of conspecifics, as is the case for other insects (Sturtevant, 1915; Greenspan and Ferveur, 2000). In *Ae. aegypti*, gustatory sensilla are located in stereotyped positions on the labella and tarsi of the legs (Chaika and Elizarov, 1971; McIver and Siemicki, 1978; Hill and Smith, 1999; Lee and Craig, 2009), although the specific expression of GRs in these tissues has not yet been reported.

Putative *Ae. aegypti* GRs have been annotated from genomic sequences and compared to previously identified insect GRs (Kent et al., 2008). In general, GRs of the two main mosquito subfamilies, Anopheline and Culicinine, share very low amino acid sequence similarity. However, a few GRs, including those related to sugar receptors or those activated by CO_2, are conserved across many insect orders including mosquitoes (Kent and Robertson, 2009; Robertson and Kent, 2009). Conservation of these GR sequences between long diverged insect species likely reflects indispensable gustatory sensitivities to a particular chemical or set of chemicals, a property that allows us to speculate as to their potential function.

Here we employed two methods to determine expression profiles of GRs in the major gustatory appendages of *Ae. aegypti*. First, we identified and quantified putative *Aaeg*GR transcripts by RNA-seq analysis; total poly-adenylated (poly(A)) RNA was isolated from the labella, as well as the pro-, meso- and metathoracic tarsi of both males and females, converted to cDNA and sequenced (Illumina). Second, we employed RT-qPCR to independently validate the RNA-seq data. We discuss the significance of the expression profiles of *Aaeg*GRs with an emphasis on those GRs with sequence orthology to functional GRs in other insects. The GRs uncovered here provide targets for high-throughput screening of chemicals for use as feeding deterrents or stimulants aimed at disruption of mosquito behavior for the protection of humans and other animals.

2. Materials and methods

2.1. Animal rearing

Ae. aegypti eggs (Orlando strain) were obtained from the Center for Medical and Veterinary Entomology, USDA, ARS in Gainesville, FL, USA. Larvae were reared at 25 °C (12-hL:12-hD) and fed with ground TetraMin® fish food. Unsexed pupae were hand-collected daily and transferred to plastic dishes (9 cm × 5.5 cm) inside small containment buckets, thus establishing 24-h age groups. Greater than 95% of adults emerged 2 days post-pupation, after which all remaining pupae were removed from containment buckets. Adult mosquitoes were fed with a 10% sucrose solution and maintained in an environmental chamber at 27 °C and 70% relative humidity under the same photoperiod as larvae. Tissues used in our studies were collected during the photophase from adult mosquitoes 6–7 days old.

2.2. RNA isolation and sequencing

For RNA sequencing, paired labella from 500 males or 500 females were carefully dissected to limit inclusion of other adjacent proboscis tissues. Samples from legs were comprised of pro-, meso-, or metathoracic tarsal segments of 400 males or 400 females. Dissected tissues were immediately stored on dry ice and mechanically ground in TRIzol® (Life Technologies, Carlsbad, CA, USA). Total RNA was isolated by RNeasy® Plus Mini Kit (Qiagen, Valencia, CA, USA), quantified on a Nanodrop ND-1000 spectrophotometer (Nano Drop Products, Wilmington, DE, USA), and sent to the Genomics Services Lab at the Hudson Alpha Institute for Biotechnology (Huntsville, AL), where samples were first assessed by Bioanalyzer (Agilent Technologies, Santa Clara, CA, USA). mRNA isolation and cDNA synthesis were completed using NEBNext® reagents (NEB, Ipswich, MA, USA) and standard protocols with custom GSL adaptors. cDNA libraries corresponding to distinct tissues were sequenced on an Illumina HiSeq2000 to generate 25 million 50 basepair, paired-end reads per sample.

2.3. Analysis of annotated and unannotated chemoreception genes

Reference genome (AaegL1, Scaffolds) and annotations (AaegL1.3) for *Ae. aegypti* were downloaded from VectorBase (http://aaegypti.vectorbase.org/GetData/Downloads/). Output Fastq Illumina files were mapped to the genome and annotated gene build with TopHat 2.0.7 (Trapnell et al., 2009). The unambiguous sequence alignment files were uploaded into the Avadis NGS software (Strand Scientific Intelligence, CA, USA), where quantification and normalization were performed. Prior to quantification using the 'Deseq' normalization method, the read list was filtered to remove duplicate, single-end, mate-filtered, mate-missing, one-mate flip, both-mate flip, and unaligned reads. Read quality metric values were sufficient to rule out low quality reads: Quality threshold $\geq$30, N's allowed in read $\leq$0, Alignment score threshold $\geq$95, Mapping quality threshold $\geq$40. Picard software (picard.sourceforge.net) was used to determine the genomic location of all reads mapping to genome assembly. Transcript expression levels for all genes are reported in values of Reads Per Kilobase per Million reads mapped (RPKM). RPKM values represent a quantitative measure of the number of corresponding 50 bp sequence reads (sequenced in both directions) for a given gene. The 4 putative protein-coding loci associated with *Aaeg*GR40 (Kent et al., 2008) are unannotated and therefore not represented in our dataset. Attempts to resolve gene models manually for read mapping were unsuccessful due to limited genomic coverage and high similarity to the related *Aaeg*GR39 locus. In addition, specific read mapping assignments for *Aaeg*GR67a, *Aaeg*GR67b and *Aaeg*GR67c were grouped as one value, as alignments for each of these transcripts were difficult to distinguish from one another by the computational approach used with the other transcripts. We assigned no specific threshold for functional expression vs. background "noise."

2.4. Quantitative RT-PCR validation of RNA sequencing

Thirteen chemoreception genes and one housekeeping gene were selected for qPCR analysis to evaluate gene expression over a dynamic range, both in predicted sequence abundance and presumed chemosensory gene function. Primer pairs were designed for each target gene to amplify a specific 100–180 basepair PCR product (Primer-BLAST Primer Designing tool, NCBI). At least one primer per set spans an intron boundary to exclude non-specific gDNA amplification.

We dissected 150 paired labella and 200 tarsi of pro-, meso and metathoracic legs from either male or female mosquitoes for each RNA extraction. Labella of both sexes were collected in biological triplicate (450 total). Total RNA was isolated as previously described. cDNA was synthesized using Superscript® III First-Strand Synthesis Supermix for qRT-PCR (Life Technologies, Carlsbad, CA, USA). Non-quantitative amplification of target genes was performed using Platinum® Taq DNA Polymerase (Life Technologies) to first confirm the correct identity and singularity of amplicons. PCR products were visualized with ethidium bromide on 2% agarose gels (Figure S1), purified with DNA Clean & Concentrator™-5 (Zymo Research, Irvine, CA, USA) and then directly sequenced to confirm

amplicon identity (data not shown) (Macrogen, Rockville, MD, USA). RT-qPCR was subsequently performed on each target gene using KiCqStart® SYBR® Green qPCR ReadyMix™ iQ (Sigma–Aldrich, St. Louis, MO, USA) and an iCycler iQ™ Real-Time PCR Detection System (Bio-Rad, Hercules, California, USA). All Ct values (Table S2) were calculated by Bio-Rad iQ5 Optical System Software (Bio-Rad, Hercules, California, USA). Reactions were performed in technical triplicate 20 μL volumes. Three-step cycles plus melt curves were used for each reaction, using an annealing temperature of 56 °C for all primers. Efficiencies for each primer set were calculated from the slope of the standard curve using the formula $E = 10^{(-1/\text{slope})}$ (Pfaffl, 2001; Rasmussen, 2001). Primer efficiencies are based on three 1:10 serial dilutions of cDNA template used in side-by-side technical triplicate reactions. Efficiencies are listed in Table S1.

Relative gene quantification was calculated as $E_{\text{target}}^{-(\text{Ct[target]} - \text{Ct [reference]})}$ for each target gene (14 total) and averaged for each replicate, both biological and technical. *Ae. aegypti* housekeeping gene Lysosomal Aspartic Protease (vectorbase ID: AAEL006169) was used to normalize Ct values between biological replicates and to root the *Y*-axis scale in comparisons of relative expression.

The relationship between the RNA-seq and RT-qPCR relative gene expression data was examined by fitting the least-squares linear regression model, RNA-seq $= b_0 + b_1 \cdot$qPCR, to data observed on the target genes, for each gender and tissue; and by testing the hypothesis of statistical equivalence of these lines with the identity line of unity slope and zero intercept. As most of the 14 target genes exhibited relatively low abundance, close to reference value 1, the observed abundance ($\sim$10) of *Aaeg*OBP11 was excluded from the statistical analyses. Including *Aaeg*OBP11 overly influenced the line estimating the RNA-seq and RT-qPCR relationship, to primarily connect the *Aaeg*OBP11 abundance to the group of closely aggregated genes near reference value 1. Excluding *Aaeg*OBP11 allowed the RNA-seq and RT-qPCR relationship to be estimated using genes with similarly low abundance values, each having similar influence on the regression line fit. Coefficients of determination (r^2) and 95% confidence intervals for intercept (b_0) and slope (b_1) (Table 1) are fit statistics. r^2 indicates the proportion of the total variability in the observed data that is explained by the regression model and $1 - r^2$, indicating how widely the gene abundance values are scattered around the model. Confidence intervals for intercept and slope were used to determine that the RNA-seq vs. RT-qPCR relationship was "not statistically different" from the line of zero intercept and unit slope. To test the hypothesis that RNA-seq and RT-qPCR abundance values were "statistically equivalent," a more statistically rigorous test was needed. To assist in assessing how similar the observed RNA-seq vs. RT-qPCR was to the identity line; the regression-based, bootstrap equivalence procedure (Robinson et al., 2005) was iteratively applied, to the data from each gender and tissue, to identify the smallest "region of similarity" that can be constructed around the observed RNA-seq and RT-qPCR data, and allow the relative gene expression as measured by RT-qPCR to be considered statistically equivalent to the measurement of relative gene expression by RNA-seq. To assist with visual assessment of the RNA-seq vs. RT-qPCR relationship, graphs were produced containing the observed data points, fitted regression line, identity line and 95% region of slop similarity. Linear regression analyses and hypothesis tests for statistical equivalence were conducted using the lm function of the stats package and the equiv.boot function of the equivalence package in the R computing environment (www.r-project.org).

Table 1
Parameter estimates and goodness-of-fit statistics for regression line fits to RNA-seq and RT-qPCR datasets.

	Least-squares regression line RNA-seq = intercept + (slope × qPCR)		r^2
	b_0	b_1	
Male labellum	0.00335 (−0.037, 0.066)	1.040 (0.99, 1.44)	0.962
Male prothoracic tarsus	−0.00132 (−0.129, 0.107)	1.189 (0.58, 1.90)	0.857
Male mesothoracic tarsus	0.02234 (−0.102, 0.147)	1.167 (0.73, 2.35)	0.806
Male metathoracic tarsus	0.00687 (−0.118, 0.080)	1.157 (0.42, 1.74)	0.913
Female labellum	−0.03121 (−0.059, 0.030)	0.955 (0.58, 1.01)	0.961
Female prothoracic tarsus	−0.00486 (−0.106, 0.073)	1.081 (0.51, 1.54)	0.923
Female mesothoracic tarsus	−0.04290 (−0.131, 0.047)	1.031 (0.30, 1.22)	0.951
Female metathoracic tarsus	−0.01106 (−0.059, 0.030)	1.003 (0.20, 1.47)	0.953

Paired values in parentheses beside Intercept (b_0) and Slope (b_1) estimates are 95% confidence intervals. r^2 (coefficient of determination) is the square the correlation of RT-qPCR estimation of relative gene abundance and that of RNA-seq, with 1 showing perfect correlation and 0 showing no correlation.

3. Results

3.1. RNA-seq analyses

Illumina based RNA-seq analysis generates sequences or "reads" of 50 bp length. Each of our analyses (labella and pro-, meso- and metathoracic tarsal segments of male or female mosquitoes) consistently yielded 18-23 million of these reads (Fig. 1). Between 8 and 12% of these reads mapped to the genome scaffold assembly for *Ae. aegypti* (AaegL1), of which $\sim$50% were subsequently mapped to annotated genes (AaegL1.3) including many putative GRs (Fig. 1; Kent et al., 2008). Thus, we focused on 85 uniquely transcribed loci, representing 87 putative *Aaeg*GRs (Fig. 2). Each *Aaeg*GR gene was assigned an RPKM value, which represents the level of expression of a given gene (see Methods). RPKM values of 3 or more represented expression well beyond that of possible background expression or "noise," although RPKM values of 1–3 may also signify functional transcripts (see Section 4.4). RPKM values for *Aaeg*GR loci in these tissues ranged from 0 (undetectable) to 80; 68 (80%) of all loci displayed quantifiable read data (Fig. 2). Labella expressed 28% of the 87 GRs at RPKM values at or above 3. Tarsal tissues expressed fewer GRs with this expression level; only 8% of the 87 GRs had RPKM values at or above 3 in any tarsal sample. Expression of putative pseudogenic GRs (Kent et al., 2008) is not reported, as RPKM values higher than 1 for pseudogenic transcripts were not observed.

Relatively high *Aaeg*GR sequence conservation was not predictive of higher expression in labella and tarsi in general; however, highly expressing *Aaeg*GRs with likely orthologs in *Anopheles gambiae* almost always demonstrated conservation in *Drosophila melanogaster* as well. Twelve out the total 40 *Aaeg*GRs with likely orthologs in *An. gambiae* had RPKM values greater than 3 in labella or tarsal tissues (Fig. 2): *Aaeg*GR3, *Aaeg*GR4, *Aaeg*GR5, *Aaeg*GR6, *Aaeg*GR7, *Aaeg*GR9, *Aaeg*GR10, *Aaeg*GR11, *Aaeg*GR14, *Aaeg*GR19c, *Aaeg*GR20d and *Aaeg*GR34. Eleven of these 12 GRs showed strong to moderate conservation in *D. melanogaster* (Kent et al., 2008), the exception being *Aaeg*GR20d. Similarly, 13 of the remaining 47 *Aaeg*GRs that lacked clear homologous relationships in *An. gambiae* showed RPKM values greater than 3 (Fig. 2): *Aaeg*GR15, *Aaeg*GR16, *Aaeg*GR17, *Aaeg*GR18, *Aaeg*GR36, *Aaeg*GR49, *Aaeg*GR55, *Aaeg*GR60, *Aaeg*GR65, *Aaeg*GR66, *Aaeg*GR72, *Aaeg*GR76 and *Aaeg*GR79.

Among the *Aaeg*GRs with the highest RPKM values were *Aaeg*GR4, *Aaeg*GR5, *Aaeg*GR6, *Aaeg*GR7, *Aaeg*GR9, *Aaeg*GR10 and *Aaeg*GR11. These 7 genes are closely related to *D. melanogaster* sugar receptors (*Dmel*GR5a, *Dmel*61a and *Dmel*GR64a-f; Kent and Robertson, 2009) and represented more than 50% of all GR loci reads for all tissues (Fig. 1). RPKM values of each of these GRs

Tissue	Raw reads	Mapped reads (genome)	High-quality reads	Read Distribution (Annotation AaegL1.3)				No. transcripts mapped (%)	Average RPKM
				Coding	UTR	Intronic	Intergenic		
Male labellum	41898982	4726228	4111816	56.46%	19.21%	2.75%	21.57%	13402 (71.4)	58.3
Male prothoracic tarsus	45017134	4447432	3853142	51.62%	21.25%	3.78%	23.35%	13379 (71.3)	51.5
Male mesothoracic tarsus	41012752	3383420	2960985	51.28%	21.39%	3.51%	23.82%	13099 (69.8)	52.5
Male metathoracic tarsus	37594444	3782617	3357323	51.79%	21.09%	3.80%	23.31%	13007 (69.3)	51.4
Female labellum	42052632	5202707	4284015	55.61%	20.09%	2.55%	21.75%	13437 (71.6)	58.9
Female prothoracic tarsus	43522544	5030526	4360730	55.18%	19.70%	3.63%	21.49%	13447 (71.7)	51.7
Female mesothoracic tarsus	40391032	3949944	3443597	50.40%	21.90%	3.62%	24.07%	13119 (69.9)	50.8
Female metathoracic tarsus	41693352	4404850	3836559	52.24%	21.69%	3.52%	22.54%	13126 (70.0)	52.5

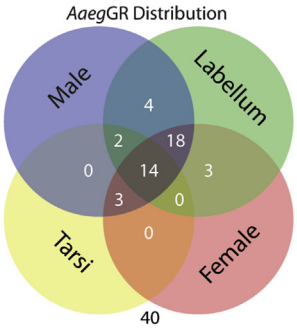

Fig. 1. RNA-seq statistics Table: Each column represents a poly-adenylated RNA sequencing metric. 'Raw reads' are the number of distinct sequences collected during sequencing. 'Mapped reads' are the number of 50 bp reads that align with *Ae. aegypti* genome (AaegL). 'High-quality reads' are the number of aligned reads with a mapping quality of at least Q20. 'Read distribution' describes the genomic location of high-quality reads as a percentage of total mapped reads for each tissue. 'No. transcripts mapped' are the number and percentage of distinct transcripts (AaegL1.3) showing a positive RPKM value. 'Average RPKM' is the average RPKM score for genes with positive values. Venn diagram: Numbers indicate total count of putative Gustatory Receptor (GR) genes that express with a minimum RPKM value of 1.0 in different tissue types. Positive tarsal expression requires RPKM value greater than or equal to 1.0 in one or more tarsal subtypes (pro-, meso- or metathoracic tarsi). Numbers in overlapping regions indicate expression that is common to inclusive distinctions, i.e. male, female, labellum, and tarsi. Number outside of all colored regions indicates putative GRs that did not show RPKM values above 1.0 for any tissue in the survey.

ranged from less than 2 to over 80 in labella, and relatively highly expressing GRs in labella also expressed relatively highly in tarsal tissues (Fig. 2). Other *Aaeg*GRs expressing at greater than 3 RPKM with functionally characterized orthologs in *D. melanogaster* included *Aaeg*GR3 (*Dmel*GR63a, required for volatile CO_2 detection), *Aaeg*GR14 (*Dmel*GR66a, required for normal caffeine and DEET detection), *Aaeg*GR19c (*Dmel*GR28b, associated with light detection and thermosensation), and *Aaeg*GR34 (*Dmel*GR43a, a fructose receptor in GRNs and neurons of the CNS).

3.2. RT-qPCR validation of RNA-seq

We next used RT-qPCR amplification of labellar and tarsal cDNA samples to validate expression trends of a small set of genes involved in chemoreception (*Aaeg*GR1, *Aaeg*GR3, *Aaeg*GR4, *Aaeg*GR9, *Aaeg*GR11, *Aaeg*GR14, *Aaeg*GR19c, *Aaeg*GR76, *Aaeg*ORCO, *Aaeg*OR4, *Aaeg*IR25a, *Aaeg*SNMP2 and *Aaeg*OBP11) and the housekeeping gene Lysosomal Aspartic Protease (*Aaeg*LAsP). Pairwise comparisons of target gene transcript abundance as determined by RNA-seq and as predicted by RT-qPCR showed very similar levels (Fig. 3). The quantities predicted by RT-qPCR never varied by more than a factor of 5 and mirrored RNA-seq data over a broad RPKM range, from 0 (*Aaeg*GR76 in labella) to 7803 (*Aaeg*OBP11 in tarsi, Table S2). All genes assigned an RPKM value of 0 by RNA-seq were predicted to be 0 or very close to that level by RT-qPCR (Fig. 3). Differences in relative abundance, like those consistently observed for *Aaeg*GR19c in tarsi (Fig. 3), may be explained by fundamental differences in RNA-seq and RT-qPCR techniques.

To further assess the concordance of the RNA-seq and RT-qPCR datasets, the degree of statistical equivalence was determined and comprehensively examined for each tissue sample (Fig. 4, Table 1). The slopes and intercepts of the 'Least-squares regression line' (Table 1; black lines, Fig. 4) indicate how closely qPCR gene expression estimates agree with actual RNA-seq read counts in each tissue, with perfect equivalence represented by lines having slope = 1 and intercept = 0 (red lines, Fig. 4). Fig. 4 illustrates the variability (r^2; Table 1) of the observed abundance values measured by RNA-seq and RT-qPCR, relative to both the least-squares (black) line and the identity (red) line. The 95% confidence intervals for intercept and slope (Table 1), contain 0 (intercept) and 1 (slope) for all tissues observed for both genders; indicating there was not evidence that any of the observed RNA-seq vs. RT-qPCR relationships were statistically different from being identical.

Increasing the statistical rigor, and testing the hypothesis that the observed RNA-seq vs. RT-qPCR relationships were statistically equivalent to the identity relationship; the area between the dashed lines (Fig. 4), bisected by the (red) identity line, illustrates the smallest "region of similarity" within which the slope of the RNA-seq vs. RT-qPCR regression line can vary and still be considered statistically equivalent to slope 1. Instead of specifying the region of similarity (i.e., slopes of the dashed lines) and then testing the hypothesis that the slope of the least-squares regression line was statistically equivalent to the identity line, we used the equivalence algorithm (iteratively) to calculate the smallest region of similarity of slope for which it could be confidently concluded that the observed RNA-seq and RT-qPCR values exhibit a relationship that was statistically equivalent to the identity. The slopes of the regions of similarity boundaries (dashed lines, Fig. 4) deviate much too widely from unity slope to be practically considered equivalent to unity; thus, our equivalence analyses detected the fundamental differences between the RNA-seq and RT-qPCR methods. However, the fit statistics for the least-squares regression lines (Table 1) indicate the relationships between the RNA-seq and RT-qPCR values observed in this study were statistically strong

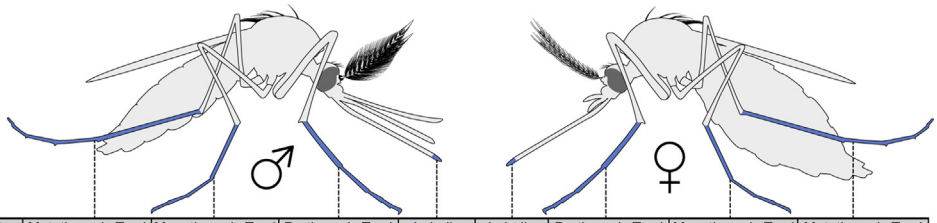

Receptor	Metathoracic Tarsi	Mesothoracic Tarsi	Prothoracic Tarsi	Labella	Labella	Prothoracic Tarsi	Mesothoracic Tarsi	Metathoracic Tarsi
GR1	0.0	0.1	0.0	0.0	0.2	0.0	0.0	0.0
GR2	0.0	0.3	0.5	0.4	0.2	0.2	0.0	0.5
GR3	0.0	0.3	0.0	9.7	13.2	0.5	0.9	1.2
GR4	6.4	13.6	14.9	32.6	42.0	8.6	7.7	6.6
GR5	0.0	0.3	0.0	1.7	4.1	0.0	0.0	0.0
GR6	2.3	2.1	4.5	3.0	3.2	0.9	2.2	1.0
GR7	6.8	17.0	16.1	77.9	66.4	11.2	11.1	9.2
GR9	3.0	5.5	7.6	80.4	79.7	5.8	5.5	5.2
GR10	0.3	0.0	0.2	34.0	28.5	0.0	0.6	0.4
GR11	0.8	1.9	1.0	10.2	8.0	0.9	1.0	0.5
GR14	0.0	0.0	0.2	43.7	36.6	0.0	0.2	0.0
GR15	0.0	0.3	0.0	4.5	5.0	0.5	0.0	0.0
GR16	0.0	0.0	0.0	11.4	17.8	0.3	0.0	0.0
GR17	0.0	0.0	0.0	9.7	10.5	0.0	0.0	0.0
GR18	0.0	0.4	0.0	6.5	6.5	0.0	0.0	0.0
GR19a	0.3	1.6	1.7	0.3	0.7	0.7	1.2	0.7
GR19b	0.0	0.0	0.0	0.0	0.0	0.3	0.0	0.0
GR19c	6.8	10.8	9.2	44.1	58.7	13.3	12.4	8.8
GR20a	0.0	0.0	0.0	1.5	1.7	0.0	0.0	0.0
GR20b	0.0	0.0	0.0	0.0	0.0	0.0	0.0	0.0
GR20d	3.0	5.6	1.8	25.3	23.1	2.3	1.4	1.7
GR20e	0.0	0.0	0.0	1.1	0.0	0.0	0.0	0.0
GR20f	0.0	0.0	0.0	0.0	0.0	0.0	0.0	0.0
GR20g	0.0	0.0	0.0	0.0	0.0	0.0	0.0	0.0
GR20h	0.0	0.0	0.0	0.0	0.0	0.0	0.0	0.0
GR20i	0.0	0.0	0.0	0.0	0.0	0.0	0.0	0.0
GR20j	0.0	0.0	0.0	0.0	0.0	0.0	0.0	0.0
GR21	0.0	0.0	0.0	0.0	0.0	0.0	0.0	0.0
GR22	0.0	0.0	0.0	0.3	1.0	0.0	0.0	0.0
GR23	0.0	0.0	0.0	0.0	0.0	0.3	0.0	0.0
GR25	0.0	2.6	1.4	0.2	1.3	1.0	0.5	0.3
GR26	0.2	0.0	0.0	2.8	1.6	0.0	0.0	0.0
GR27	1.8	2.2	0.9	2.0	0.0	0.0	0.0	0.0
GR28	0.0	0.0	0.0	0.0	0.0	0.0	0.0	0.0
GR29	0.0	0.0	0.0	0.0	0.0	0.0	0.0	0.0
GR31c	0.0	0.0	0.0	0.0	0.0	0.0	0.0	0.0
GR32	0.0	0.0	0.3	0.2	0.3	0.2	0.3	0.0
GR33a	0.6	0.0	0.0	0.1	0.0	0.0	0.0	0.0
GR33b	0.0	0.0	0.4	0.1	0.0	0.1	0.0	0.0
GR34	0.0	1.1	0.1	1.5	6.2	1.1	0.7	0.5
GR35	1.0	2.7	2.7	0.9	2.4	1.1	2.2	1.2
GR36	0.2	2.0	3.1	0.3	0.4	0.5	1.0	1.1
GR37	0.0	0.0	0.0	1.0	1.4	0.0	0.0	0.0
GR39a	0.0	0.0	0.0	0.0	0.0	0.0	0.0	0.0
GR39e	0.4	0.0	0.3	2.8	0.1	0.0	0.0	0.0
GR41	0.0	0.0	0.0	0.3	0.8	0.0	0.3	0.0
GR42	0.0	0.0	0.3	0.7	1.8	0.0	0.0	0.0
GR43	0.9	1.5	1.1	1.8	0.0	0.4	0.0	0.0
GR44	0.0	0.0	0.0	0.0	0.5	0.0	0.0	0.0
GR45	0.0	0.0	0.1	2.0	1.1	0.0	0.0	0.3
GR46	0.0	1.0	0.4	0.9	1.5	0.2	0.0	0.3
GR47	0.0	0.0	0.0	0.0	0.4	0.0	0.0	0.0
GR49	0.3	0.7	1.6	3.2	3.0	1.0	0.0	0.6
GR51	0.0	0.0	0.0	0.0	0.0	0.0	0.0	0.0
GR53	0.0	0.0	0.0	0.5	0.3	0.0	0.0	0.0
GR54	0.0	0.0	0.0	1.1	1.2	0.0	0.0	0.0
GR55	0.0	0.0	0.0	3.2	3.1	0.0	0.0	0.0
GR56	0.0	0.0	0.0	0.5	1.2	0.0	0.0	0.0
GR57	0.0	0.0	0.0	1.2	0.8	0.0	0.0	0.0
GR58	0.0	0.0	0.0	0.0	0.0	0.0	0.0	0.0
GR59	0.3	0.0	0.0	0.0	0.0	0.0	0.0	0.0
GR60	0.0	0.0	0.0	12.3	12.9	0.0	0.0	0.0
GR61	0.0	0.0	0.0	0.0	0.1	0.0	0.0	0.0
GR62	0.0	0.0	0.0	0.0	0.0	0.0	0.0	0.0
GR63	0.0	0.0	0.0	0.0	0.1	0.0	0.0	0.0
GR64	0.0	0.0	0.0	0.0	0.0	0.2	0.2	0.0
GR65	0.0	0.0	0.0	11.1	13.2	0.0	0.0	0.0
GR66	0.0	0.0	0.0	4.5	10.1	0.0	0.0	0.0
GR67a,b,c	0.0	0.0	0.0	0.1	0.2	0.0	0.0	0.0
GR67d	0.0	0.0	0.0	1.1	0.0	0.0	0.0	0.0
GR67f	0.0	0.0	0.0	1.1	2.0	0.0	0.0	0.0
GR68a	0.0	0.0	0.0	0.0	0.0	0.0	0.0	0.0
GR68b	0.0	0.0	0.0	0.0	0.0	0.0	0.0	0.0
GR69	0.0	0.0	0.0	0.0	0.0	0.0	0.0	0.0
GR70	0.0	0.0	0.0	0.0	0.0	0.0	0.0	0.0
GR71	0.0	0.0	0.0	0.2	0.0	0.0	0.0	0.0
GR72	1.4	2.5	1.8	7.0	6.8	2.1	1.8	1.4
GR73	0.0	0.0	0.0	0.5	0.0	0.4	0.3	0.0
GR74a	0.0	0.0	0.0	0.0	0.0	0.0	0.0	0.0
GR74b	0.0	0.0	0.0	0.0	0.0	0.0	0.0	0.0
GR74c	0.0	0.0	0.0	0.0	0.3	0.0	0.0	0.0
GR76	0.0	3.3	10.0	0.0	0.0	7.3	1.3	0.5
GR77	0.0	0.0	0.3	0.2	0.5	0.0	0.0	0.0
GR78	0.0	0.0	0.0	0.3	0.4	0.0	0.0	0.0
GR79	0.0	0.0	0.0	3.6	5.1	0.0	0.0	0.0

Fig. 2. RPKM values for putative Gustatory Receptors in Ae. aegypti Top: Dissected tissues from males (left) and females (right) are indicated by blue shading. Table: Cells report RPKM values for each Gustatory Receptor annotation or gene cluster. Numerical values are rounded to the nearest tenth. Heat-map color intensity is capped at RPKM value 10 in order to better distinguish values between 1 and 10. All values greater than 10 display maximum color intensity.

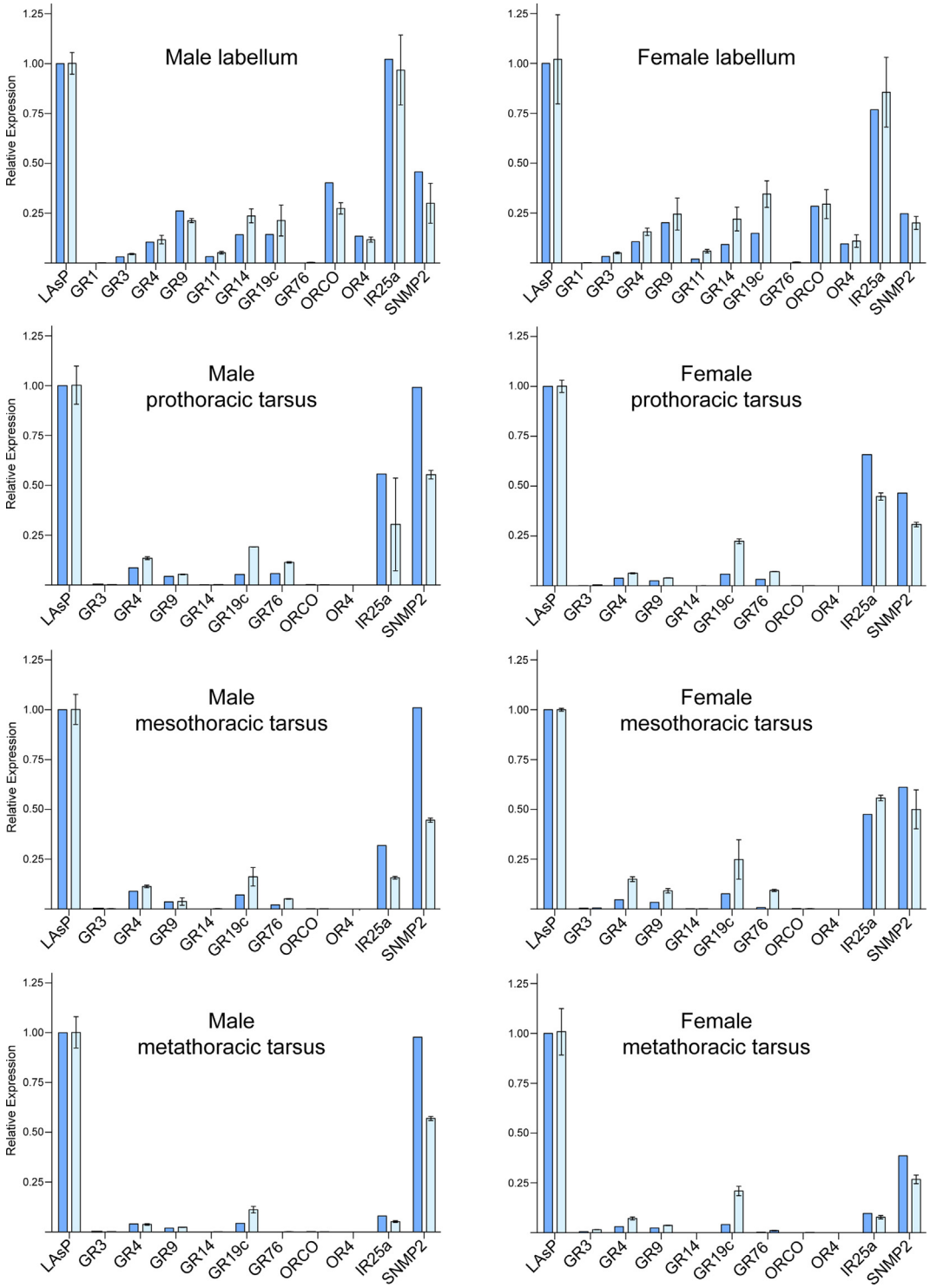

Fig. 3. RT-qPCR validation of RNA-seq data in labella and tarsi Each chemoreception gene of the horizontal axis is represented by two data columns. The left column represents relative expression as determined by RNA-seq; RPKM values of chemoreception genes were divided by that of *Aaeg*LAsP to generate numerical proportions in each tissue. The right column represents relative expression as determined by RT-qPCR. First, biological replicate Ct values for labella genes were normalized using *Aaeg*LAsP as a standard. Second, technical replicate (9 for labella, 3 for tarsi) Ct values for each gene were used to calculate relative expression values ($E_{target}^{-(Ct[target] - Ct[reference])}$). The error bars indicate standard deviation of individually calculated relative expression values. RNA-seq and RT-qPCR datasets for each tissue were compared in separate analyses ('Methods', Fig. 4).

enough to provide supporting and complementary information beneficial to making conclusions about our study objectives. Quantitative estimation of transcript abundance by RT-qPCR of 12 chemoreception genes and the housekeeping gene *Aaeg*LAsP support the RNA-seq read quantification data most strongly for all female tissue and male labella, and less strongly for male tarsi.

4. Discussion

Gustatory receptors provide mosquitoes with the capability to detect chemical signals important for feeding, oviposition and conspecific recognition. Moreover, the feeding deterrent DEET both stimulates *Ae. aegypti* labellar GSNs (Sanford et al., 2013) and

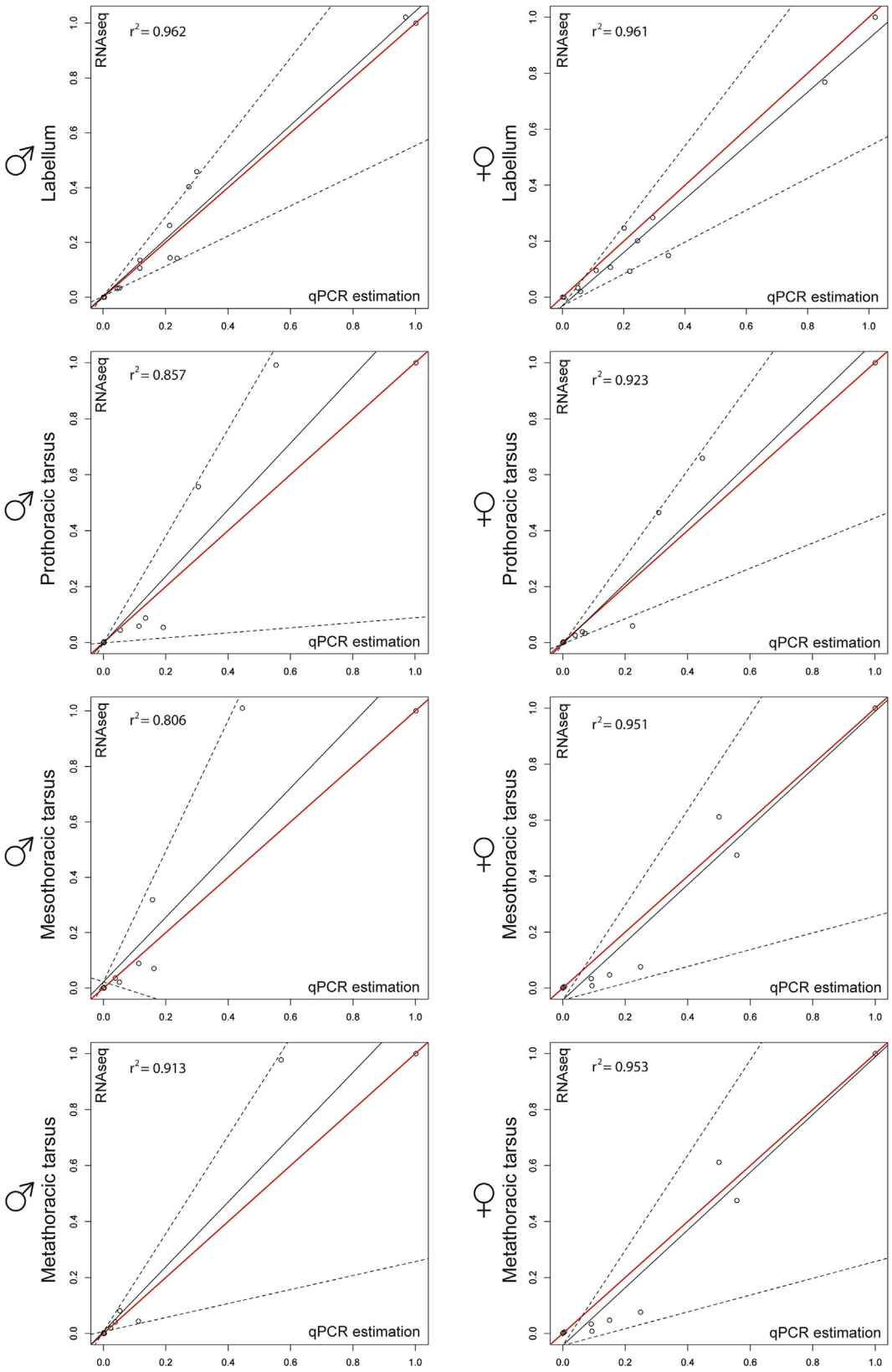

Fig. 4. Statistical equivalence plots of RNA-seq and RT-qPCR datasets The vertical axes represent relative gene abundance as demonstrated by RNA-seq data, with a value of 1 being attributed to housekeeping gene *Aaeg*LAsP and all other gene expression being reported relative to this value. The horizontal axes represent relative gene abundance as predicted by RT-qPCR, with a value of 1 being attributed to housekeeping gene *Aaeg*LAsP and all other gene expression being reported relative to this value. Red lines represent exact equivalence. Dashed lines represent boundaries of the "region of similarity" for slope, calculated by the statistical equivalence algorithm (Robinson et al., 2005). Solid black lines represent the least-squares regression of RT-qPCR equivalence to RNA-seq quantification for the 12 target genes and *Aaeg*LAsP housekeeping gene, each represented by circle data point.

evokes avoidance behavior in anosmic *Ae. aegypti* (DeGennaro et al., 2013). Here we discuss specific *Aaeg*GRs likely involved in these and other behaviors and their expression profiles in the primary gustatory appendages.

Using RNA-seq, we detected 41 *Aaeg*GRs expressing in labella and 19 *Aaeg*GRs expressing in at least one tarsal sample, 16 of which were common to both tissue types (Venn diagram, Fig. 1; Fig. 2). We then validated this sequencing using RT-qPCR to estimate relative expression levels of a small set of chemoreception genes (Fig. 3). A statistical comparison of RNA-seq and RT-qPCR data for *Ae. aegypti* chemoreception genes demonstrated a similar trend (Table 1) between the data collected by each method, but not exact equivalence (Fig. 4). As previously stated, the two techniques are limited by different chemistries, and thus did not produce identical data. However, relative expression trends of all genes tested are broadly reflected in side-by-side comparisons (Fig. 3).

4.1. Expression of conserved AaegGRs

*Aaeg*GR1, *Aaeg*GR2 and *Aaeg*GR3 represent the most highly conserved GRs in insects (Jones et al., 2007; Kent et al., 2008; Robertson and Kent, 2009). *Aaeg*GR1 and *Aaeg*GR3 are each required for normal CO_2 activation of sensory neurons on the maxillary palps (Erdelyan et al., 2012), a function conserved in *D. melanogaster* (orthologs *Dmel*GR21a and *Dmel*GR63a, Jones et al., 2007). A function has not been attributed to the *Aaeg*GR1 paralog *Aaeg*GR2, although *Aaeg*GR2 is also expressed in the maxillary palp and well conserved (Kent et al., 2008; Kent and Robertson, 2009). Interestingly, while significant expression of *Aaeg*GR3 (RPKM = 13.2 female, 9.7 male) occurs in the labella, *Aaeg*GR1 (RPKM = 0.2 female, 0.0 male) and *Aaeg*GR2 (RPKM = 0.2 female, 0.4 male) expression are barely detectable in this tissue (Figs. 2 and 3). *Aaeg*GR1 and *Aaeg*GR3 are thought to function as hetero-dimeric sensors of volatile CO_2, however no function has been attributed to *Aaeg*GR3 singularly or in combination with GRs other than *Aaeg*GR1. Proboscis ablation does not appear to significantly affect CO_2 initiated host-seeking behavior in *An. stephensi* (Maekawa et al., 2011); therefore, it is unlikely that *Aaeg*GR3 expression in the labellum is related to CO_2 detection. It is possible *Aaeg*GR3 is either non-functional though transcribed in this context or has a yet to be described role.

All seven of the putative sugar receptors identified by sequence homology (Kent et al., 2008) are expressed in the labella of both sexes (Figs. 2 and 3). This expression is consistent with sugar GRs from *D. melanogaster* (Clyne et al., 2000; Scott et al., 2001; Dunipace et al., 2001 Chyb et al., 2003; Dahanukar et al., 2007). The most highly expressing GRs within this clade in labella (*Aaeg*GR4, *Aaeg*GR7 and *Aaeg*GR9) also express highly in tarsi relative to all other putative *Aaeg*GRs. Since insect GRs may function as hetero-dimers or multimers (Jiao et al., 2008; Moon et al., 2009; Lee et al., 2009; Weiss et al., 2011) with particular GRs serving as ubiquitous co-receptors to subsets of other GRs with more narrowly tuned chemical sensitivities, these three *Aaeg*GRs are the most salient candidate sugar co-receptors. Sugar perception in mosquitoes is crucial for the identification of suitable nutritive sources for feeding (Galun and Fraenkel, 1957; Salama, 1967; Briegel and Kaiser, 1973; Clements, 1992). Sugar stimulation of tarsi induces labella probing behaviors in both males and females leading to active sugar feeding (Frings and Hamrum, 1950; Feir et al., 1961; Pappas and Larsen, 1978; Clements, 1992). Both physiological responses of sugar sensitive of hairs on the tarsi and labella, and feeding behavior are well documented (Salama, 1966; Pappas and Larsen, 1976; Angioy et al., 1982). Our data confirm the expression of all conserved sugar receptors in the labella and demonstrate expression of at least some of them in legs. This strongly suggests that the *Aaeg*GRs of this group are required for normal physiological and behavioral responses of mosquitoes to sugar stimuli.

An even more highly conserved sugar sensitive GR, *Dmel*GR43a, is required for labellar and tarsal GRN responses to fructose as well as normal feeding behavior involving sensing of hemolymph fructose levels in the CNS in *D. melanogaster* (Miyamoto et al., 2012). Interestingly, *Aaeg*GR34, the likely ortholog of *Dmel*GR43a, shows about 4-fold enrichment in female labella with respect to male labella (Fig. 2). If this GR serves as a fructose receptor in mosquitoes, this differential expression between the sexes may reflect a sensory adaptation to fructose in females.

*Aaeg*GR14 is the fourth most abundant *Aaeg*GR transcript in the labella of both sexes in our survey and is the only putative bitter receptor based on sequence homology (Kent et al., 2008). Unlike its *D. melanogaster* ortholog *Dmel*GR66a, *Aaeg*GR14 is not expressed in tarsi (Fig. 2), noting that all leg expression data for *Dmel*GR66a to date is promoter-based and not directly determined from localized RNA (Scott et al., 2001; Dunipace et al., 2001; Bray and Amrein, 2003; Moon et al., 2006). *Dmel*GR66a is required (along with *Dmel*GR32a and *Dmel*GR33a) but not sufficient for activation of *D. melanogaster* GRNs and aversive feeding response elicited by the deterrent DEET (Lee et al., 2010). *Dmel*GR66a is also involved in the detection of caffeine, a bitter stimulus, and is expressed in every bitter sensitive GRN in the labellum (Moon et al., 2006, 2009). Both the orthology of *Aaeg*GR14 with *Dmel*GR66a and its relatively high expression suggest it may be involved in the detection of aversive substances in *Ae. aegypti*. Indeed, a recent electrophysiological study identified a GRN housed within sensilla on the labella of *Ae. aegypti* that responded to bitter quinine as well as DEET and other known insect repellents (Sanford et al., 2013). Subsequently, avoidance responses specifically associated with contact chemoreception of DEET were observed in behavioral studies of transgenic *Ae. aegypti* in which the olfactory co-receptor Orco was mutated (DeGennaro et al., 2013). These behaviors were separate from avoidance of volatile DEET cues, a caveat only indirectly tested in prior feeding assays involving insect repellents (Bar-Zeev and Schmidt, 1959; Klun et al., 2006).

Significant expression (RPKM range 6–59) of *Aaeg*GR19c, the third most abundant transcript in our survey, is evident in the labella and tarsi of both sexes (Fig. 2). Alternative splice forms *AaegGR*19a and *AaegGR*19b show much lower RPKM values in legs and labella (RPKM range 0–1.7). The alternatively spliced *Aaeg*GR19 locus is orthologous to a similarly spliced locus in *D. melanogaster, Dmel*GR28b (Kent et al., 2008). Three of the five splice variants of the *Dmel*GR28b(A-E) locus show atypical GR expression patterns in addition to commonly observed peripheral sensory neuron expression. Promoter-driven reporter and transcript expression is evident for these three genes in Johnston's organ, the base of the aristae, campaniform sensilla of the wing, neurons within the CNS, oenocytes and neurons of the abdominal wall and gut (Thorne and Amrein, 2008; Park and Kwon, 2011). In addition, the *Dmel*GR28b locus is required for light-induced responses of class IV dendritic arborization neurons in larvae (Xiang et al., 2010) and the *Dmel*GR28b-D transcript confers thermosensitivity in the antennae and aristae of *D. melanogaster* (Ni et al., 2013). *Dmel*GR28b-E is the most downstream of the genes in the *Dmel*GR28 locus and is only expressed in labella and tarsi. Similarly, *Aaeg*GR19c is the most downstream of the genes in the *Aaeg*GR19 locus and is expressed in the labella and tarsi (Figs. 2 and 3). Whether these consistencies reflect conservation of expression pattern or function between the respective loci remains a topic for future investigations.

4.2. Expression of non-conserved AaegGRs

Thirteen *Ae. aegypti*-specific GRs showed expression values above 3 RPKM in any tissue (Fig. 2). Without strong homology to previously characterized GRs, we are unable to speculate as to their possible functions. A majority (33/38) of the GR promoters driving expression in *D. melanogaster* labella label bitter sensitive GSNs (Weiss et al., 2011); all exceptions being well-described sugar receptors labeling sugar sensitive GRNs. Furthermore, large expansions of bitter sensitive GRs have been proposed for the silkmoth *Bombyx mori* (Wanner and Robertson, 2008). Thus, it is possible that a majority of the *Ae. aegypti*-specific GRs expressing in labella are involved in the detection of bitter substances.

Unlike the other GRs in this group, *Aaeg*GR76 is only expressed in tarsi (Fig. 2); being the third most abundant GR in male prothoracic tarsi and the fourth most abundant GR in female prothoracic tarsi. *Aaeg*GR76 may be involved in a non-labellar gustatory modality. Furthermore, *Aaeg*GR76 RPKM values of 10.0 in male and 7.3 in female prothoracic tarsi contrast lower values in mesothoracic tarsi and zero values in metathoracic tarsi for both sexes (Fig. 2). These tarsal expression patterns may reflect sensory pathways unique to a single tarsal type, thus highlighting differences in chemoreception function between tarsal types.

4.3. Sex-specific AaegGR expression

Sex-specific expression biases greater than 2-fold among *Aaeg*GRs in the labella and tarsi tissues are numerous (Fig. 2; male-enriched: *Aaeg*GR20e, *Aaeg*GR27, *Aaeg*GR36, *Aaeg*GR39e, *Aaeg*GR43; female-enriched: *Aaeg*GR5, *Aaeg*GR22 *Aaeg*GR34, *Aaeg*GR44, *Aaeg*GR56). These differences in expression may indicate involvement of these GRs in sex-specific recognition of social cues or in the case of females, blood-host attractants. Identifying *Aaeg*GRs that elicit neuronal responses to non-volatile sex-specific cuticular hydrocarbons could provide a basis for uncovering attractive or repulsive neuronal circuitry in the tarsi and labella of *Ae. aegypti.* Likewise, *Aaeg*GRs that elicit neuronal responses to non-volatile blood-host cues could provide clues to neuronal circuitry involved in the mosquito's choice to bite. Female, but not male, *Ae. aegypti* take host blood-meal to supplement egg production (Clements, 1992); therefore, it is possible that female-enriched *Aaeg*GR5, *Aaeg*GR22, *Aaeg*GR44 or *Aaeg*GR56 are involved in the reception of blood-host cues.

The relatively balanced expression between males and females of all other *Aaeg*GRs does not exclude them from mediating sex-specific behaviors, as differences in peripheral GRN circuitry rather than GRN receptor repertoire are sometimes more predictive of sex-linked behavior in insects (Villella and Hall, 2008; Lu et al., 2012; Thistle et al., 2012). The neuronal signals elicited by *Aaeg*GRs expressing equally in both sexes may be differentially interpreted by downstream circuitry that is sex-specific.

4.4. Challenges of sequencing AaegGRs

Surprisingly, only 8–12% of total RNA-seq reads mapped to the genome scaffold assembly of *Ae. aegypti* for labella and tarsi samples (Fig. 1). This proportion was much lower than those observed in prior RNA-sequencing of mosquito chemosensory tissue as between 90 and 94% reads mapped to the genome assembly for *An. gambiae* for antennal preparations (Pitts et al., 2011); however, it was closer to proportions reported for *Ae. aegypti* whole-body (less than 40%; Bonizzoni et al., 2011) and larva (47%; Paris et al., 2012). Even so, a more recent developmental study reports between 80 and 95% read mapping to the *Aedes* genome, depending on the tissue type (Akbari et al., 2013). Global BLASTs (blastn) were performed on the four most redundant, non-mapped 50 basepair reads to test for possible contamination in all eight tissue samples (data not shown) (pers. comm. Nripesh Prasad, Hudson-Alpha Institute for Biotechnology); for all tests, reads produced high similarity hits with insect genes, the most similar genes being from mosquito species. Therefore, it is unlikely that the unmapped reads correspond to contaminant nucleotides. Rather, it is likely the majority of raw reads for labella and tarsi correspond to actively transcribing transposable elements (~50% of *Ae. aegypti* genome; Nene et al., 2007) that are not well represented in the genome assembly.

A reasonable distribution of genomic locations was observed for reads that did map to the *Ae. aegypti* genome (Fig. 1). At least half of these reads mapped to coding regions for each tissue sample, suggesting we have obtained an accurate cross-section of expressed genes in all tissues. Non-mapped reads displayed a similar GC content to that of mapped reads (45%). We also mapped all unmapped reads to the 16,665 basepair mitochondrial genome (Behura et al., 2011) to rule out an abundance of mitochondria in our dissected tissue types. Only 2% of our unmapped reads mapped to this genome for the female labella sample (~900,000 reads; data not shown), therefore this is not a consideration. To date there are no other RNA-seq datasets for insect tarsi or labella, thus direct comparisons of read mapping percentages for these tissue types are not possible. A few instances of low genome mapping percentages have been reported for insect RNA-seq datasets, but these do not represent a majority of published data (14.4% for late stage *D. melanogaster* embryos, Daines et al., 2011).

In another study by our group, RNA-seq analysis of the maxillary palps of female *Ae. aegypti* of the same age and strain yielded raw reads of which ~80% mapped to the genome assembly (data not shown). These reads were mapped to the same genome assembly file using the same software parameters presented here. The starting RNA quality was identical as determined by Bioanalyzer (data not shown) and average read quality was actually lower than that of reads used in this study (Table S3). Therefore, our relatively low mapping percentage may reflect a unique transcriptional feature of labella and tarsi tissues in *Ae. aegypti*.

Low GR transcript levels observed in insects have made identification of specific GR genes challenging without the use of promoter-driven reporters (Isono and Morita, 2010). RNA-seq is sensitive enough to identify these rare transcripts, even as their expression levels approach that of background "noise" (Wang et al., 2009). In the labella and tarsi, the primary gustatory organs of adult *Ae. aegypti*, 28% (24/85) of the putative *Aaeg*GR loci displayed RPKM values higher than 3, a level proposed to represent expression well above background levels associated with non-functional or otherwise leaky genomic regions (Ramsköld et al., 2009). Lower RPKM values of 1–3 account for another 22% (19/85) of *Aaeg*GRs in these tissues. The remaining 50% of putative *Aaeg*GRs are below the threshold of 1 RPKM, which approaches levels indistinguishable from background or non-significant expression. Nevertheless, we cannot rule out the possibility that these transcripts, if truly expressed, may produce functional GRs in the labella or legs of the mosquito, albeit in as few as one cell or in a very low copy number. This is less of a concern in labella tissue, as there are about 30 large gustatory sensilla tightly distributed over a majority of the outer surface, each innervated with 3–5 GRNs (Chaika and Elizarov, 1971; Lee and Craig, 2009). GRNs within sensilla on the tarsi of mosquito legs represent a relatively smaller portion of the total cells comprising these appendages. Females and males have approximately 100 and 60 tarsal gustatory sensilla, respectively; each sensillum is innervated with 4–5 GRNs (McIver and Siemicki, 1978). Thus, there are less than 500 total GRNs in female tarsi and less than 300 GRNs in male tarsi in which GRs are likely

expressed. Moreover, taking *D. melanogaster* tarsal GRNs as a model (Dunipace et al., 2001; Scott et al., 2001), only a small subset of these neurons may be expressing a given GR. Thus, it may be necessary to target more specifically the gustatory organs of tarsi for RNA extraction in order to better resolve the expression of *Aaeg*GRs.

While our survey reveals expression of at least half of the putative *Aaeg*GRs in labella and tarsi, a subset of the remaining *Aaeg*GRs likely express in other tissues including the labrum, cibarial organ and perhaps elsewhere (Lee, 1974; Clements, 1992). Indeed, *Aaeg*GR expression has been reported in the maxillary palp (Erdelyan et al., 2012; Bohbot et al., 2013), and in *An. gambiae*, GR expression is evident in both the antennae and maxillary palps (Pitts et al., 2011). In *D. melanogaster*, GRs express in neuronal tissues of the antennae, Johnston's organ, wings, genitalia, pharynx and CNS (Clyne et al., 2000; Dunipace et al., 2001; Scott et al., 2001; Ikeya et al., 2002; Thorne and Amrein, 2008; Ejima and Griffith, 2008). Promoter-based expression studies also indicate *Dmel*GR expression in digestive and somatosensory tissues (Thorne and Amrein, 2008; Park and Kwon, 2011). Several of these *Dmel*GRs are required for physiology and behavior associated with these tissues. Additionally, some mosquito GRs may be expressed in larval or pupal stages and have specific functions associated with an aquatic environment. Future GR expression profiling in *Ae. aegypti* should extend to these tissues, in addition to those surveyed here.

4.5. Future considerations

*Aaeg*GRs expressed in labella and tarsal tissues mediate discrimination of many contact chemical stimuli, and those well-conserved GRs may exhibit predictable sensitivities, some of which are directly linked to host-selection or assessment of sugar sources. Most *Aaeg*GRs are divergent however, and greater resolution as to their expression pattern is needed to better understand their roles. The *Aaeg*GRs identified here are potential guideposts to resolve *Aaeg*GR co-expression in single sensory neurons by double labeling with RNA probes or promoter-driven reporters. The *Aaeg*GRs showing highest expression levels in our survey, like those related to sugar GRs, may be tested first to assess the feasibility of single cell labeling in labella. Such an expression map would help determine the combinatorial code for *Aaeg*GR function in GRNs with sugar or bitter sensitivities. *Aaeg*GRs also provide suitable subjects for future *in vivo* gene disruption or *ex vivo* heterologous expression studies, and are targets for the disruption or modification of gustatory-mediated behavior in mosquitoes. Several techniques have recently been used to successfully alter target genes in *Ae. aegypti* (Aryan et al., 2013a, 2013b; DeGennaro et al., 2013), thus opening the door to comprehensively studying the function of individual *Aaeg*GRs.

Acknowledgments

The authors thank Dr. Shawn E. Levy and Nripesh Prasad of the Genomics Services Lab at the Hudson-Alpha Institute for Biotechnology for RNA sequencing and data analyses; Dr. Hugh Robertson, Department of Entomology, University of Illinois at Urbana-Champaign for *Ae. aegypti* putative GR sequences and Dr. Jonathan D. Bohbot of our group for the mosquito illustration in Fig. 2 and graphical abstract. We are grateful to Dr. Rick Jones USDA, ARS, GIFVL, Beltsville, MD for advice and Drs. Richard Vogt, Department of Biological Sciences, University of South Carolina and Daniel Strickman for critical review of manuscript. We also thank Kevin Nyberg, Department of Biology, University of Maryland for assistance with bioinformatic screens. This work was supported in part by a grant to J.C.D. from the Deployed War Fighter Protection (DWFP) Research Program funded by the Department of Defense through the Armed Forces Pest Management Board (AFPMB).

Appendix A. Supplementary data

Supplementary data related to this article can be found at http://dx.doi.org/10.1016/j.ibmb.2013.10.005.

References

Akbari, O.S., Antoshechkin, I., Amrhein, H., Williams, B., Diloreto, R., Sandler, J., Hay, B.A., 2013. The developmental transcriptome of the mosquito Aedes aegypti, an invasive species and major arbovirus vector. G3: Genes Genom. Genet.. http://dx.doi.org/10.1534/g3.113.006742.

Al-Anzi, B., Tracey Jr., W.D., Benzier, S., 2006. Response of *Drosophila* to wasabi is mediated by painless, the fly homolog of mammalian TRPA1/ANKTM1. Curr. Biol. 16, 1034–1040.

Angioy, A.M., Liscia, A., Pietra, P., Stoffolano Jr., J.G., 1982. The labellar and tarsal chemosensilla in *Anopheles maculipennis atroparvus* Van Thiel: electrophysiological and morphological observation. Boll. Soc. Ital. Biol. Sper. 58, 1330–1336.

Aryan, A., Anderson, M.A.E., Myles, K.M., Adelman, Z.M., 2013a. TALEN-based gene disruption in the dengue vector Aedes aegypti. PLoS One 8, e60082.

Aryan, A., Anderson, M.A.E., Myles, K.M., Adelman, Z.M., 2013b. Germline excision of transgenes in *Aedes aegypti* by homing endonucleases. Scientific Rep. 3, 1603.

Bar-Zeev, M., Schmidt, C.H., 1959. Action of a repellent as indicated by a radioactive tracer. J. Econ. Entomol. 52, 268–269.

Barban, V., Munoz-Jordan, J.L., Santiago, G.A., Mantel, N., Girerd, Y., Gulia, S., Claude, J.B., Lang, J., 2012. Broad neutralization of wild-type dengue virus isolates following immunization in monkeys with a tetravalent dengue vaccine based on chimeric yellow fever 17D/dengue viruses. Virology 429, 91–98.

Beatty, M.E., Beutels, P., Meltzer, M.I., Shepard, D.S., Hombach, J., et al., 2011. Health economics of dengue: a systematic literature review and expert panel's assessment. Am. J. Trop. Med. Hyg 84, 473–488.

Behura, S.K., Lobo, N.F., Haas, B., deBruyn, B., Lovin, D.D., Shumway, M.F., Pulu, D., Romero-Severson, J., Nene, V., Severson, D.W., 2011. Complete sequences of mitochondria genomes of *Aedes aegypti* and *Culex quinquefasciatus* and comparative analysis of mitochondrial DNA fragments inserted in the nuclear genomes. Insect Biochem. Mol. Biol. 41, 770–777.

Bhatt, S., Gething, P.W., Brady, O.J., Messina, J.P., Farlow, A.W., Moyes, C.L., et al., 2013. The global distribution and burden of dengue. Nat. Lond. 496, 504–507.

Bidlingmayer, W.L., Hem, D.G., 1980. The range of visual attraction and the effect of competitive visual attractants upon mosquito flight. Bull. Entomol. Res. 70, 321–342.

Bohbot, J.D., Durand, N.F., Vinyard, B.T., Dickens, J.C., 2013. Functional development of the octenol response in *Aedes aegypti*. Front. Physiol. 4, 1–8.

Bonizzoni, M., Dunn, W.A., Campbell, C.L., Olson, K.E., Dimon, M.T., Marinotti, O., James, A.A., 2011. RNA-seq analyses of blood-induced changes in gene expression in the mosquito vector species, *Aedes aegypti*. BMC Genomics 12, 82.

Bowen, M.F., 1991. The sensory physiology of host-seeking behavior in mosquitoes. Annu. Rev. Entomol. 36, 139–158.

Bray, S., Amrein, H., 2003. A putative Drosophila pheromone receptor expressed in male-specific taste neurons is required for efficient courtship. Neuron 39, 1019–1029.

Briegel, H., Kaiser, C., 1973. Life-span of mosquitoes under laboratory conditions. Gerontologia 19, 240–249.

Cameron, P., Hiroi, M., Ngai, J., Scott, K., 2010. The molecular basis for water taste in *Drosophila*. Nat. Lond. 465, 91–95.

Chaika, S.Y., Elizarov, Y.A., 1971. Electron microscopic investigation of the labellar trichoid sensilla of mosquito *Aedes aegypti*. In: Contribution to the Lst All-union Symposium on Insect Chemoreception, pp. 67–73.

Chen, Z., Wang, Q., Wang, Z., 2010. The amiloride-sensitive epithelial Na^+ channel PPK28 is essential for *Drosophila* gustatory water reception. J. Neurosci. 30, 6247–6252.

Chyb, S., Dahanukar, A., Wickens, A., Carlson, J.R., 2003. *Drosophila* Gr5a encodes a taste receptor tuned to trehalose. Proc. Nat. Acad. Sci. U.S.A 100, 14526–14530.

Clements, A.N., 1992. The Biology of Mosquitoes. Chapman & Hall, London, Glasgow, New York, Tokyo, Melbourne, Madras.

Clyne, P.J., Warr, C.G., Carlson, J.R., 2000. Candidate taste receptors in *Drosophila*. Sci. Wash 287, 1830–1834.

Croset, V., Rytz, R., Cummins, S.F., Budd, A., Brawand, D., Kaessmann, H., Gibson, T.J., Benton, R., 2010. Ancient protostome origin of chemosensory ionotropic glutamate receptors and the evolution of insect taste and olfaction. PLoS Genet. 6, e1001064.

Dahanukar, A., Lei, Y.T., Kwon, J.Y., Carlson, J.R., 2007. Two Gr genes underlie sugar reception in Drosophila. Neuron 56, 503–516.

Daines, B., Wang, H., Wang, L., Li, Y., Han, Y., Emmert, D., Gelbart, W., Wang, X., Li, W., Gibbs, R., Chen, R., 2011. The *Drosophila melanogaster* transcriptome by paired-end RNA sequencing. Genome Res. 21, 315–324.

Debboun, M., Strickman, D., 2013. Insect repellents and associated personal protection for a reduction of human disease. Med. Vet. Entomol. 27, 1–9.

DeGennaro, M., McBride, C.S., Seeholzer, L., Nakagawa, T., Dennis, E.J., Goldman, C., Jasinskiene, N., James, A.A., Vosshall, L.B., 2013. orco mutant mosquitoes lose

strong preference for humans and are not repelled by volatile DEET. Nat. Lond. 498, 487–491.
Dunipace, L., Meister, S., McNealy, C., Amrein, H., 2001. Spatially restricted expression of candidate taste receptors in the *Drosophila* gustatory system. Curr. Biol. 11, 822–835.
Ejima, A., Griffith, L.C., 2008. Courtship initiation is stimulated by acoustic signals in *Drosophila melanogaster*. PLoS One 3, e3246.
Erdelyan, C.N.G., Mahood, T.H., Bader, T.S.Y., Whyard, S., 2012. Functional validation of the carbon dioxide receptor genes in *Aedes aegypti* mosquitoes using RNA interference. Insect Mol. Biol. 21, 119–127.
Feir, D., Lengy, J.I., Owen, W.B., 1961. Contact chemoreception in the mosquito *Culiseta inornata*: sensitivity of the tarsi and labella to sucrose and glucose. J. Insect Physiol. 6, 13–20.
Fischler, W., Kong, P., Marella, S., Scott, K., 2007. The detection of carbonation by the *Drosophila* gustatory system. Nat. Lond. 448, 1054–1057.
Frings, H., Hamrum, C.L., 1950. The contact chemoreceptors of adult yellow fever mosquitoes, Aedes aegypti. J. New York Entomol. Soc. 58, 133–142.
Galun, R., Fraenkel, G., 1957. Physiological effects of carbohydrates in the nutrition of a mosquito, *Aedes aegypti* and two flies *Sarcophaga bullata* and *Musca domestica*. J. Cellu. Compar. Physiol. 50, 1–23.
Greenspan, R.J., Ferveur, J.F., 2000. Courtship in *Drosophila*. Annu. Rev. Genet. 34, 205–232.
Guzman, M.G., Halstead, S.B., Artsob, H., Buchy, P., Farrar, J., et al., 2010. Dengue: a continuing global threat. Nat. Rev. Microbiol, S7–S16.
Hill, S.R., Smith, J.J.B., 1999. Consistent pattern in the placement of taste sensilla on the labellar lobes of *Aedes aegypti*. Int. J. Insect Morphol. Embryol. 28, 281–290.
Ikeya, T., Galic, M., Belawat, P., Nairz, K., Hafen, E., 2002. Nutrient-dependent expression of insulin-like peptides from neuroendocrine cells in the CNS contributes to growth regulation in *Drosophila*. Curr. Biol. 12, 1293–1300.
Isono, K., Morita, H., 2010. Molecular and cellular designs of insect taste receptor system. Front. Cellu. Neurosci. 4, 1–16.
Jiao, Y., Moon, S.J., Wang, X., Ren, Q., Montell, C., 2008. Gr64f is required in combination with other gustatory receptors for sugar detection in *Drosophila*. Curr. Biol. 18, 1797–1801.
Jones, W.D., Cayirlioglu, P., Kadow, I.G., Vosshall, L.B., 2007. Two chemosensory receptors together mediate carbon dioxide detection in *Drosophila*. Nat. Lond. 445, 86–90.
Kent, L.B., Walden, K.K.O., Robertson, H.M., 2008. The Gr family of candidate gustatory and olfactory receptors in the yellow-fever mosquito *Aedes aegypti*. Chem. Senses 33, 79–93.
Kent, L.B., Robertson, H.M., 2009. Evolution of the sugar receptors in insects. BMC Evol. Biol. 9, 41.
Kim, S.H., Lee, Y., Akitake, B., Woodward, O.M., Guggino, W.B., Montell, C., 2010. Drosophila TRPA1 channel mediates chemical avoidance in gustatory receptor neurons. Proc. Nat. Acad. Sci. U.S.A 107, 8440–8445.
Klun, J.A., Khrimian, A., Debboun, M., 2006. Repellent and deterrent effects of SS220, picaridin, and DEET suppress human blood feeding by *Aedes aegypti, Anopheles stephensi*, and *Phlebotomus papatasi*. J. Med. Entomol. 43, 34–39.
Klun, J.A., Kramer, M., Debboun, M., 2013. Four simple stimuli that induce host-seeking and blood-feeding behaviors in two mosquito species, with a clue to DEET's mode of action. J. Vector Ecol. 38, 143–153.
Laarman, J.J., 1958. The host-seeking behavior of anopheline mosquitoes. Trop. Geogr. Med. 10, 293–305.
Lee, R., 1974. Structure and function of the fascicular stylets, and the labral and cibarial sense organs of male and female *Aedes aegypti*. Quaest. Entomol. 10, 187–215.
Lee, R.M.K.W., Craig, D.A., 2009. Fine structure of the sense organs on the labella and labium of the mosquito *Aedes aegypti*. Open Entomol. J. 3, 7–17.
Lee, Y., Moon, S.J., Montell, C., 2009. Multiple gustatory receptors required for the caffeine response in Drosophila. Proc. Nat. Acad. Sci. U.S.A 106, 4495–4500.
Lee, Y., Kim, S.H., Montell, C., 2010. Avoiding DEET through insect gustatory receptors. Neuron 67, 555–561.
Lin, H., Mann, K.J., Starostina, E., Kinser, R.D., Pikielny, C.W., 2005. A *Drosophila* DEG/ENaC channel subunit is required for male response to female pheromones. Proc. Nat. Acad. Sci. U.S.A 102, 12831–12836.
Liu, L., Leonard, A.S., Motto, D.G., Feller, M.A., Price, M.P., Johnson, W.A., Welsh, M.J., 2003. Contribution of *Drosophila* DEG/ENaC genes to salt taste. Neuron 39, 133–146.
Lu, B., LaMora, A., Sun, Y., Welsh, M.J., Ben-Shahar, Y., 2012. ppk23-Dependent chemosensory functions contribute to courtship behavior in *Drosophila melanogaster*. PLoS Genet. 8, e1002587.
Maekawa, E., Aonuma, H., Nelson, B., Yoshimura, A., Tokunaga, F., Fukumoto, S., Kanuka, H., 2011. The role of proboscis of the malaria vector mosquito *Anopheles stephensi* in host-seeking behavior. Parasites Vect. 4, 10.
McIver, S., Siemicki, R., 1978. Fine structire of tarsal sensilla of *Aedes aegypti*. J. Morphol. 155, 137–155.
Miyamoto, T., Slone, J., Song, X., Amrein, H., 2012. A fructose receptor functions as a nutrient sensor in the *Drosophila* brain. Cell 151, 1113–1125.
Miyazaki, T., Ito, K., 2010. Neural architecture of the primary gustatory center of *Drosophila melanogaster* visualized with GAL4 and LexA enhancer-trap systems. J. Comp. Neurol. 518, 4147–4181.
Mitri, C., Soustelle, L., Framery, B., Bockaert, J., Parmentier, M.L., Grau, Y., 2009. Plant insecticide L-canavanine repels *Drosophila* via the insect orphan GPCR DmX. PLoS Biol. 7, e1000147.
Moon, S.J., Köttgen, M., Jiao, Y., Xu, H., Montel, C., 2006. A taste receptor required for the caffeine response in vivo. Curr. Biol. 16, 1812–1817.
Moon, S.J., Lee, Y., Jiao, Y., Montell, C., 2009. A *Drosophila* gustatory receptor essential for aversive taste and inhibiting male-to-male courtship. Curr. Biol. 19, 1623–1627.
Nene, V., Wortman, J.R., Lawson, D., Haas, B., Kodira, C., Tu, Z.J., et al., 2007. Genome sequence of *Aedes aegypti*, a major arbovirus vector. Sci. Wash 316, 1718–1723.
Ni, L., Bronk, P., Chang, E.C., Lowell, A.M., Flam, J.O., Panzano, V.C., Theobald, D.L., Griffith, L.C., Garrity, P.A., 2013. A gustatory receptor paralogue controls rapid warmth avoidance in *Drosophila*. Nature. http://dx.doi.org/10.1038/nature12390.
Pappas, L.G., Larsen, J.R., 1976. Gustatory hairs on the mosquito, *Culiseta inornata*. J. Exp. Zool. 196, 351–360.
Pappas, L.G., Larsen, J.R., 1978. Gustatory mechanisms and feeding in the mosquito, *Culiseta inornata*. Physiol. Entomol. 3, 115–119.
Paris, M., Melodelima, C., Coissac, E., Tetreau, G., Reynaud, S., David, J., Despres, L., 2012. Transcription profiling of resistance to Bti toxins in the mosquito *Aedes aegypti* using next-generation sequencing. J. Invert. Pathol. 109, 201–208.
Park, J.H., Kwon, J.Y., 2011. Heterogeneous expression of *Drosophila* gustatory receptors in enteroendocrine cells. PloS One 6, e29022.
Peterson, D.G., Brown, A.W.A., 1952. Studies of the responses of the female *Aedes* mosquito. III. The response of *Aedes aegypti* to a warm body and its radiation. Bull. Entomol. Res. 42, 535–541.
Pfaffl, M., 2001. A new mathematical model for relative quantification in real-time RT-PCR. Nucl. Acids Res. 29, e45.
Pitts, R.J., Rinker, D.C., Jones, P.L., Rokas, A., Zwiebel, L.J., 2011. Transcriptome profiling of chemosensory appendages in the malaria vector *Anopheles gambiae* reveals tissue- and sex-specific signatures of odor coding. BMC Genomics 12, 271.
Ramsköld, D., Wang, E.T., Burge, C.B., Sandberg, R., 2009. An abundance of ubiquitously expressed genes revealed by tissue transcriptome sequence data. PLoS Comput. Biol. 512, e1000598.
Rasmussen, R., 2001. Quantification on the LightCycler instrument. In: Meurer, S., Wittwer, C., Nakagawara, K. (Eds.), Rapid Cycle Real-time PCR: Methods and Applications. Springer, Heidelberg, pp. 21–34.
Robertson, H.M., Warr, C.G., Carlson, J.R., 2003. Molecular evolution of the insect chemoreceptor gene superfamily in *Drosophila melanogaster*. Proc. Nat. Acad. Sci. U.S.A 100, 14537–14542.
Robertson, H.M., Kent, L.B., 2009. Evolution of the gene lineage encoding the carbon dioxide receptor in insects. J. Insect Sci. 9, 19.
Robinson, A.P., Duursma, R.A., Marshall, J.D., 2005. A regression-based equivalence test for model validation: shifting the burden of proof. Tree Physiol. 25, 903–913.
Sabchareon, A., Wallace, D., Sirivichayakul, C., Limkittikul, K., Chanthavanich, P., Suvannadabba, S., Jiwariyavej, V., et al., 2012. Protective efficacy of the recombinant, live-attenuated, CYD tetravalent dengue vaccine in Thai schoolchildren: a randomised, controlled phase 2b trial. Lancet 380, 1559–1567.
Salama, H.S., 1966. The function of mosquito taste receptors. J. Insect Physiol. 12, 1051–1060.
Salama, H.S., 1967. Nutritive values and taste sensitivity to carbohydrates for mosquitoes. Mosq. News 27, 32–35.
Sanford, J.L., Shields, V.D.C., Dickens, J.C., 2013. Gustatory receptor neuron responds to DEET and other insect repellents in the yellow-fever mosquito, Aedes aegypti. Naturwiss 100, 269–273.
Scott, K., Brady, J.R., Cravchik, A., Morozov, P., Rzhetsky, A., Zuker, C., Axel, R., 2001. A chemosensory gene family encoding candidate gustatory and olfactory receptors in *Drosophila*. Cell 104, 661–673.
Stocker, R., 1994. The organization of the chemosensory system in *Drosophila melanogaster*: a review. Cell Tiss. Res. 275, 3–26.
Sturtevant, A.H., 1915. A sex-linked character in *Drosophila repleta*. Amer. Nat. 49, 189–192.
Thistle, R., Cameron, P., Ghorayshi, A., Dennison, L., Scott, K., 2012. Contact chemoreceptors mediate male-male repulsion and male-female attraction during *Drosophila* courtship. Cell 149, 1140–1151.
Thorne, N., Chromey, C., Bray, S., Amrein, H., 2004. Taste perception and coding in *Drosophila*. Curr. Biol. 14, 1065–1079.
Thorne, N., Amrein, H., 2008. Atypical expression of *Drosophila* gustatory receptor genes in sensory and central neurons. J. Comp. Neurol. 506, 548–568.
Trapnell, C., Pachter, L., Salzberg, S.L., 2009. TopHat: discovering splice junctions with RNA-seq. Bioinformatics 25, 1105–1111.
Villella, A., Hall, J.C., 2008. Neurogenetics of courtship and mating in *Drosophila*. Adv. Genet. 62, 67–183.
Wallace, D., Canouet, V., Garbes, P., Wartel, T.A., 2013. Challenges in the clinical development of a dengue vaccine. Curr. Opin. Virol.. http://dx.doi.org/10.1016/j.coviro.2013.05.014.
Wang, Z., Gerstein, M., Snyder, M., 2009. RNA-seq: a revolutionary tool for transcriptomics. Nat. Rev. Genet. 10, 57–63.
Wang, Z., Singhvi, A., Kong, P., Scott, K., 2004. Taste representations in the Drosophila brain. Cell 117, 981–991.
Wanner, K.W., Robertson, H.M., 2008. The gustatory receptor family in the silkworm moth Bombyx mori is characterized by a large expansion of a single lineage of putative bitter receptors. Insect Mol. Biol. 17, 621–629.
Weiss, L.A., Dahanukar, A., Kwon, J.Y., Banerjee, D., Carlson, J.R., 2011. The molecular and cellular basis of bitter taste in *Drosophila*. Neuron 69, 258–272.
Xiang, Y., Yuan, Q., Vogt, N., Looger, L.L., Jan, L.Y., Jan, Y.N., 2010. Light-avoidance-mediating photoreceptors tile the *Drosophila* larval body wall. Nat. Lond. 468, 921–926.
Zhang, Y.V., Ni, J., Montell, C., 2013. The molecular basis for attractive salt-taste coding in *Drosophila*. Sci. Wash 340, 1334–1338.